JOURNAL OF KUFA–PHYSICS
journal.uokufa.edu.iq/index.php/jkp/index | ISSN: 2077–5830

Preparation and comparison of performance for CuO Nanoparticles and CuO/TiO_2 Nanocomposite and their applications in solar cell

*** Ghanem Abdulnabi** **Amer Musa Juda**

Chemistry Department, Faculty of Science, Kufa University, Najaf, Iraq.

*Corresponding Author E-mail: ghanemn.alkreete@student.uokufa.edu.iq

ARTICLE INF

Article history:
Received: 10 DEC, 2022
Revised: 01 JEN, 2022
Accepted: 03 JEN, 2023
Available Online: 00 JUN, 2023

Keywords:

CuO/TiO_2
Nanocomposite
Hydrothermal
DSSCs

ABSTRACT

Nanostructures of metal oxides of CuO, and TiO_2 were prepared by the hydrothermal method. Also, CuO/TiO_2 nanocomposites were prepared by the hydrothermal technique using an equal ratio of 1:1 The properties of the prepared compounds were investigated through Field Emission Scanning Electron Microscopy FE-SEM, Transmission Electron Microscopy TEM, X-Ray Diffraction. The images of FE-SEM have confirmed that the prepared TiO_2 , CuO, and nanoparticles were structured as Nanoparticles, Spherical, and CuO/ TiO_2 nanocomposites which were mixed in an equal ratio were structured as rocks-like structures. The results of the X-ray diffraction indicated the presence of CuO, and TiO_2 as (monoclinic structures, Tetragonal) respectively. with the average crystallite sizes,(13.10,8.65 and 10.12)nm, for CuO , TiO_2 and CuO/TiO_2 respectively. The optical properties of the prepared nanoparticles CuO , TiO_2 , and CuO/TiO_2 were studied through UV-Vis Spectroscopy. The optical band gap of the prepared products was determined by UV-Visible spectrophotometry and was found to be 2.1, 3.0, and 2.8 eV for TiO_2, CuO, NPs, and CuO /TiO_2 nanocomposites respectively. Dye-sensitized solar cells (DSSCs) fabricated based on TiO2, CuO, NPs, and CuO /TiO_2 nanocomposites are casted onto (FTO) substrates (front electrode), while the back electrode is carbon/FTO-glass substrate. Two types of natural dyes were used in this study. Chlorophyll pigment in green leek and anthocyanin red pigment in cochineal pomegranate whereas iodine/ iodide KI/I2 is used as the electrolyte solution. The solar cells efficiency rates (1.51,0.74 and 0.94) for CuO, TiO_2 NPs, and CuO /TiO_2 nanocomposites/ are chlorophyll pigments present in green leek respectively. and The solar cells efficiency rates (1.20,0.558 and 0.88) for CuO, TiO_2 Nps, and CuO/TiO_2 nanocomposites/ anthocyanin pigment present in red pomegranate respectively

DOI: https://doi.org/10.31257/2018/JKP/2023/v15.i01.10696

تحضير ومقارنة اداء المركب النانوي CuO والمتراكب النانوي CuO/TiO_2 وتطبيقها في الخلايا الشمسية

غانم عبدالنبي كاظم عامر موسى جودة

قسم الكيمياء ـ كلية العلوم ـ جامعة الكوفة ـ النجف ـ العراق

الـــخُـــلاصـــة

تم تحضير أكاسيد المعادن ذات الهياكل النانوية لـ TiO_2 و CuO من خلال الطريقة الحرارية المائية. تم أيضًا تحضير المتراكب النانوي CuO/TiO_2 باستخدام التقنية الحرارية المائية باستخدام نسبة متساوية (١: ١) تم فحص خصائص المركبات المحضرة من خلال الفحص المجهري الإلكتروني الماسح (FE-SEM) وحيود الأشعة السينية XRD .أكدت صور FE-SEM أن TiO_2 و CuO منظمة على شكل (نانوية ،كروية) . بينما شكل المتراكب النانوي CuO /TiO_2 بنسبة (١:١) منظمة على شكل (هيكل يشبه الصخور). أشارت نتائج حيود الأشعة السينية إلى وجود كل من CuO و TiO_2 على شكل (هيكل أحادي الميل ، رباعي الزوايا) على التوالي مع متوسط أحجام البلورات (31.10،8,65 و 10.12) نانومتر ، لـ CuO و TiO_2 و CuO / TiO_2 على التوالي. تمت دراسة الخواص البصرية للجسيمات النانوية CuO و TiO_2 و CuO / TiO_2 من خلال التحليل الطيفي للأشعة المرئية وفوق البنفسجية. تم تحديد فجوة النطاق البصري للمنتجات المحضرة بواسطة القياس الطيفي المرئي للأشعة فوق البنفسجية وتم العثور على (2.1، 3.0 و2.8) الكترون فولت لمركبات TiO_2 و CuO و NPs و CuO / TiO_2 على التوالي.

تم تصنيع الخلايا الشمسية الصبغية (DSSCs) على أساس المركبات النانوية CuO, TiO_2 و CuO /TiO_2 كإلكترونات مضادة. تم تحضير TiO_2 CuO و CuO /TiO_2 على ركائز (FTO) (القطب الأمامي) بينما يكون القطب الخلفي هو عبارة عن ركيزة من الكربون / الزجاج FTO. تم استخدام نوعين من الأصباغ الطبيعية في هذه الدراسة. صبغة الكلوروفيل في الكراث الأخضر وصبغة الأنثوسيانين الحمراء في الرمان القرمزي بينما يستخدم اليود / اليود KI / I_2 كمحلول إلكتروليت. معدلات كفاءة الخلايا الشمسية هي معدلات كفاءة الخلايا الشمسية هي (1.51, 0.94,0.74)لـ TiO_2,CuO و CuO/TiO_2 باستخدام صبغة الكلوروفيلالخضراء في الكراث رعلى التوالي. ومعدلات كفاءة الخلايا الشمسية (0.88,0.558,1.20) لـ TiO_2,CuO, CuO/TiO_2 باستخدام صبغة الانثوسيايين الحمراء في الرمان على التوالي.

الكلمات المفتاحية:

متراكب نانوي

CuO/TiO_2 –

حراري مائي

DSSs –

1. INTRODUCTION

Nanomaterials have emerged as a remarkable class of materials with a wide variety of samples and at least one dimension in the 1 to 100 nm range. The logical design of nanoparticles allows for exceptionally high surface areas[1]. It is possible to create nanomaterials with exceptional magnetic, electrical, optical, mechanical, and catalytic capabilities that differ significantly from those of their bulk counterparts. By carefully regulating the size, shape, synthesis conditions, and appropriate functionalization, the properties of nanomaterials can be tailored to meet specific needs[2]. A semiconductor-based photovoltaic device known as a dye solar cell DSSC converts solar and artificial radiation directly into clerical current. In DSSC, the two functions are

separated from each other unlike in conventional systems, where semiconductors are responsible for both charge carrier separation and transport as well as light absorption. In a typical DSSC, the sensitizer bound to the surface of a broadband gap semiconductor absorbs light [3]. This hybrid device, also known as the Grätzel cell, was initially introduced to the scientific community in 1991 by Brian O'Regan and Michael Grätzel in their foundational work, which described a device composed of sensitive TiO2 nanoparticles with an energy conversion efficiency of 7.1% [2]. DSSCs are probably[4]. nanoparticles of CuO. One of the transition metal oxide nanoparticles that have become highly sought-after materials for numerous applications is CuO (Copper Oxide) nanoparticles. The CuO nanoparticles are p-type oxide semiconductors with a bandgap of 1.2–1.5 eV, in contrast to metal oxides, which typically have a very wide band gap . Solar cells are one application for nanoparticles. One potential source of sustainable energy is solar power or solar cells[5]. TiO_2 is one of the most widely used semiconductors because of its non-toxicity, stability in aqueous solutions, excellent quantum efficiencies, and acceptable bandgap, TiO_2 is one of the most widely used semiconductor photocatalysts [6]. As shown in Figure 1, when TiO_2 is illuminated, the electrons are promoted from the valence band to the conduction band, leaving an electron vacancy or hole in VB. However, this only occurs if the photon energy is equivalent to or higher than the band gap energy of the photocatalyst, in our case, TiO_2. In addition, ultraviolet light irradiation of TiO_2 photocatalysts causes photoexcitation due to the band gap energy of the TiO_2 photocatalyst, which is 3.2 eV (=385 nm) for rutile 3.0 eV (=410 nm)[7].

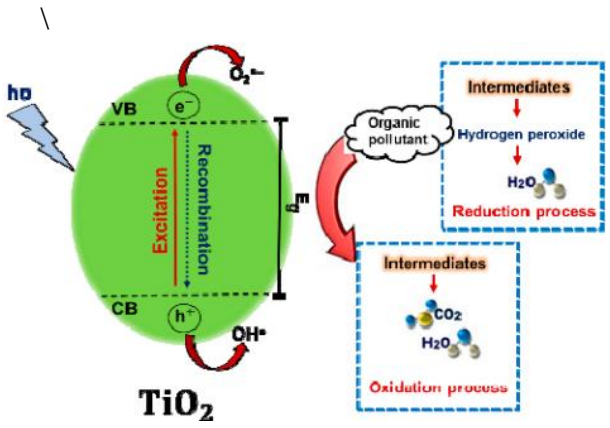

Figure 1: Schematic illustration of typical photocatalysis over TiO_2[7].

Five components make up the DSSC: two transparent conductive substrates, a layer of nanostructured titanium dioxide, a layer of platinum, dye molecules, and an electrolyte. TheTiO_2 and platinum nanostructures are applied as thin coatings to transparent conductive surfaces, respectively. This sort of solar cell's mechanism is an exact reproduction of the steps in a plant's photosynthesis cycle [33]. The dye molecule is excited from its ground state to its excited state through the absorption of light, as shown in Figure (2)[8].

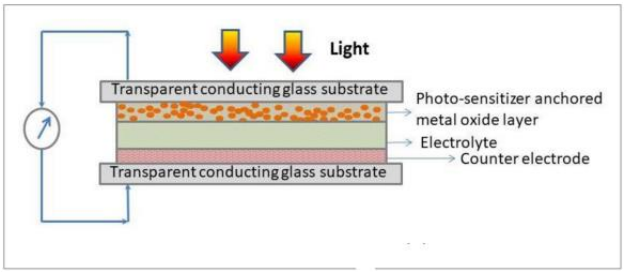

Figure 2: Schematic configuration of a dye-sensitized solar cell[9].

2. EXPERIMENTAL PART

2.1 Synthesis of CuO Nanopartecles and CuO /TiO_2 Nanocomposites

The, CuO, TiO_2 Nanoparticles and CuO /TiO_2 nanocomposites were prepared by hydrothermal method by using $CuSO_4.5H_2O$, and TTIP Ti (OC_3H_7) 4 as a source of Cu^{+2}, and Ti^{+4} Ions were purchased from Merck[10], [11]. The hydrothermal method was used for TiO_2/CuO synthesis 2. 26 g of titanium tetra

isopropoxide Ti[OCH(CH_3)$_2$]4 and 2 g of $CuSO_4$ .5H_2O were dissolved in 100 mL of distilled water and 0.8 M of NaOH were added to the solution medium until the pH reaches 85, and the stirring continued until a homogeneous solution was obtained. Then, the solution was transferred to the Teflon autoclave reactor and kept in the oven for 20 hours at 140°C. The sample was filtered and rinsed with distilled water and then ethanol multiple times before being dried in a vacuum at 60oC for 4 hours after the autoclave had naturally cooled to room. Then, the solution was transferred to the Teflon autoclave reactor and kept in the oven for 20 hours at 150C°.The. After the autoclave had naturally cooled to room temperature, the sample was filtered and washed with distilled water and then ethanol several times before being dried in a vacuum at 50 C^o for 5 hours [12]**.**

2.2 Characterization methods

The properties of the prepared compounds are investigated through Field Emission Scanning Electron Microscopy FE-SEM, Transmission Electron Microscopy typ (TESCAN BRNO-Mira3LMU/ Tescan) TEM (Philips em 208s,100Kv) and X-Ray Diffraction typ (6000/Shimadzu, Japan). All chemicals in this work were purchased from Merck company and used without further purification such as NaOH (98%), TTIP Ti (OC3H7) 4 (99%)and $CuSO_4$ .5H_2O(98%). The efficiency of the solar cell was calculated by Programmable Keithley electrometer (2400) with the relation

$$FF = \frac{J_{max} \times V_{max}}{J_{sc} \times V_{oc}} \qquad (1)$$

where: J_{SC} is the short circuit current, V_{OC} is the open-circuit voltage, J_{MAX} is the maximum current, V_{MAX} is the maximum voltage [13].

3. RESULTS AND DISCUSSIONS

3.1 X-ray diffraction analysis

Figure (2) shows the XRD peaks of CuO NPs at 100 C^o (PH=10) nanoparticles appeared at (33.11°, 36.23°, 38.94° ,54.36°, 60.24°, 61.24° and 68.34°) corresponding to (101, 004, 200, 105, 211, 204, 220 and 215.) respectively, which indicates the formation of a monoclinic structure CuO crystal structure with space group (C2/c), monoclinic structure, conforms to the monoclinic structure (JCPDS No. 80-1268) with average crystalline size (8.6) nm [14, 15]. shows the XRD peaks of TiO2 NPs prepared by hydrothermal PH=9 at 400 C^o appeared at(33.24°, ,36.34° ,39.44° °,49.84°, 54.26°, 63.04°, 69.90°, 25,24° and 33.2 4°) corresponding(101 , 110 ,101, 004 ,111, 200,1 05 and 211). respectively which indicates the (TiO2) tetragonal structure, with the space group (I41/amd), This finding is consistent with the standard (JCPD 73-1764) data .with average crystallines ize (7.10)nm [16].Nonetheless, no additional peaks were identified that could have been caused by the contaminant. The nano sized TiO_2 has a very high crystallinity, as evidenced by the sharp peaks [17]. Figure (5) shows the sharp and strong peaks suggest that the obtained nanocomposite has high crystalline character. The JCPDS card numbers, 80-1268 and73-1764 all corroborated the monoclinic structure of CuO and the tetragonal structure of TiO_2 in the CuO/TiO_2 nanocomposites [18].

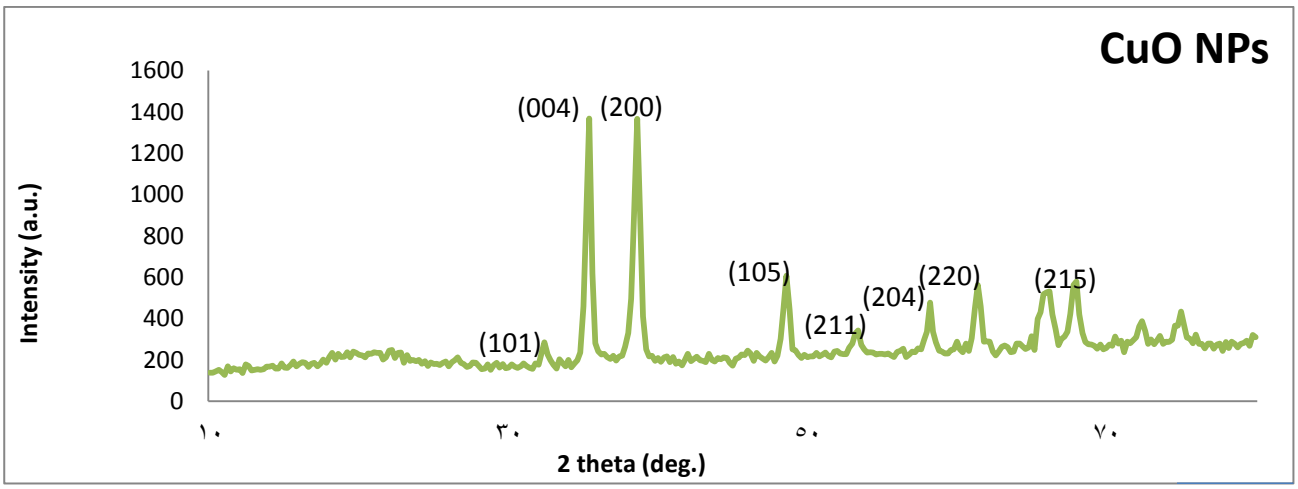

Figure 3: XRD patterns CuO NPs at 100 ^{o}C prepared by hydrothermal method.

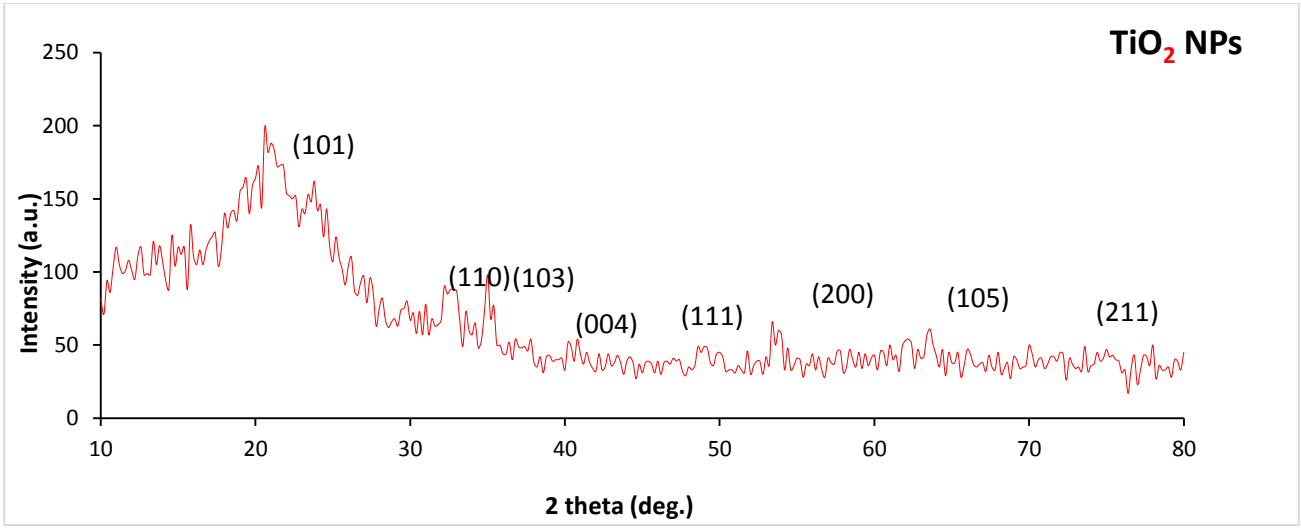

Figure 4: XRD patterns of TiO_2 NPs prepared by hydrothermal method.

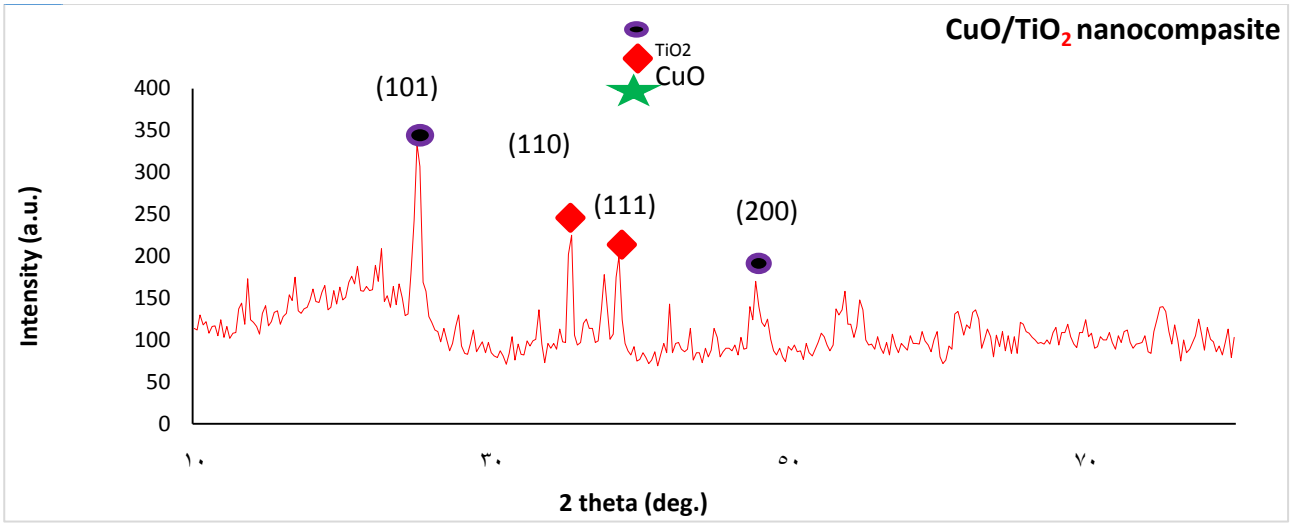

Figure 5: XRD patterns of CuO/TiO_2 NPs prepared by hydrothermal method

3.2 FESEM Analysis of CuO,TiO_2 Nanopartecles and CuO /TiO_2 Nanocomposites

The hydrothermal approach produced CuO NPs with a particle size range of 40.69 to 60.67 nm and a spherical-like structure at 100 oC for two hours at PH=10, as shown in figure 6 (A-

D). Due to the fact that the crystalline character of CuO increased with increasing the reaction temperature to 100 °C, as demonstrated by the XRD results [19]**.** The FE-SEM images of the TiO_2 nanoparticles NPs generated by the hydrothermal technique at PH are shown in Figure 7(A-D) (8). It is obvious that different materials and particles have varied morphologies. Zones of TiO_2, which are the bright spots in figure 7(A–D), can be attributed to both free Ti and O_2 particles. The particle size was about (33.71 to 33.95) nm with nanoparticle [20]**.** Figure 8 A–D), shows the FE-SEM images of the CuO/TiO_2 nanocomposite to the dark areas were the Ti particles embedded into Cu particles in bright areas. Since the Cu content was too low, its particles were hard to identify. Both phases indicate the form of the CuO/TiO_2 (cubic). These phases are CuO and TiO_2 which are formed as thermally induced martensites and varied in terms of thickness and orientation. The CuO formed as a spherical-like phase, while the TiO_2 formed as a cubic-like phase between the CuO/ TiO_2 and the particle size of 34 to 51 nm [21]**.**

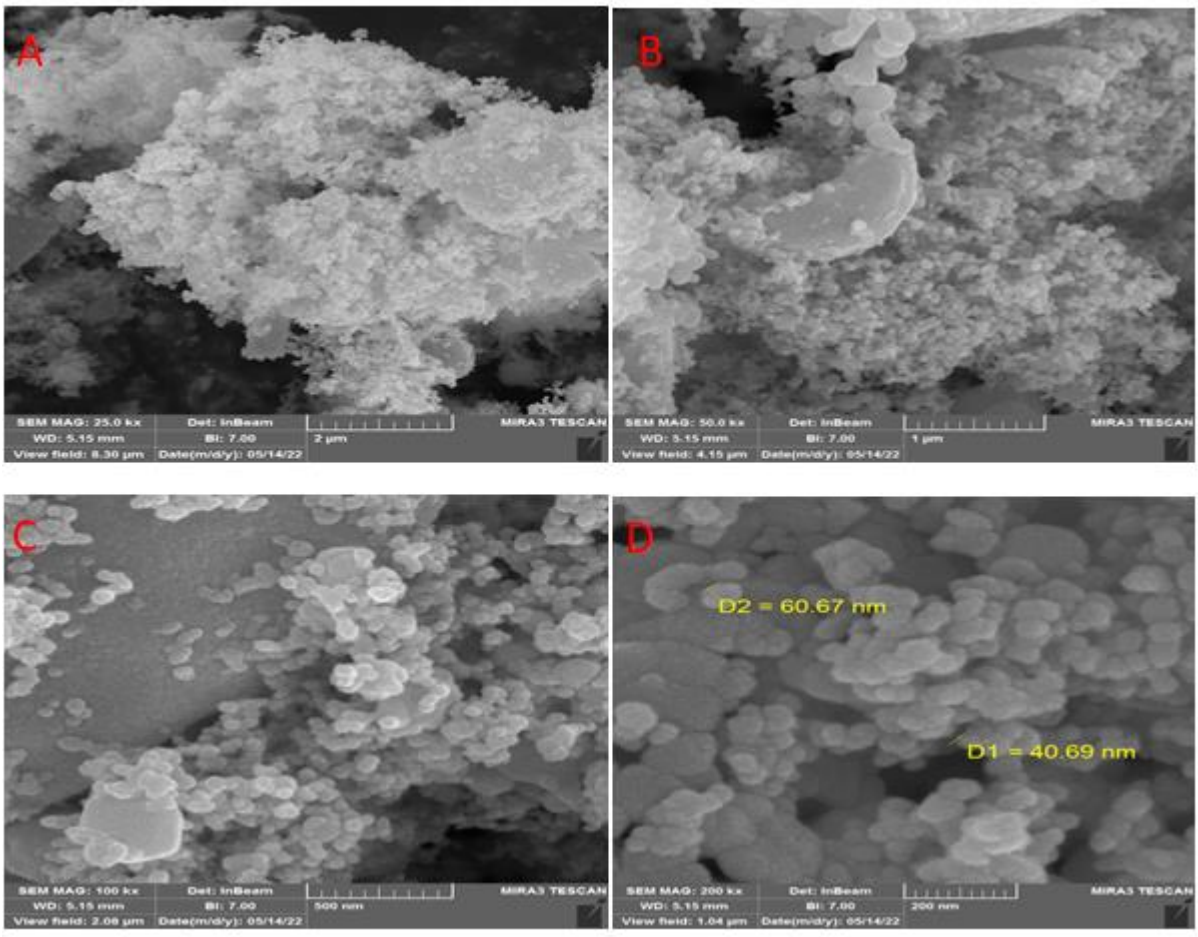

Figure 6: FE-SEM images of CuO NPs prepared by hydrothermal method at 100 ^{o}C for 2h at PH=10.

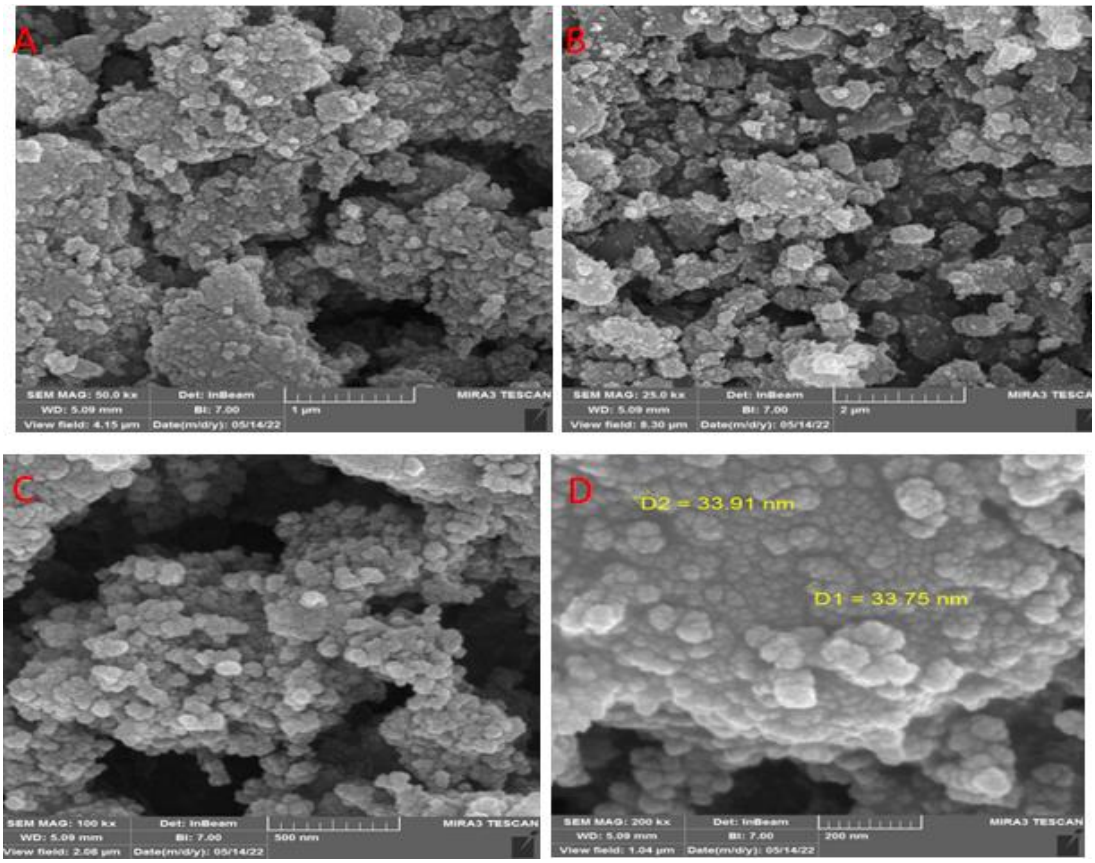

Figure 7: FE-SEM images of TiO_2 NPs prepared by hydrothermal method at 400 ^oC for 2h at PH=8.

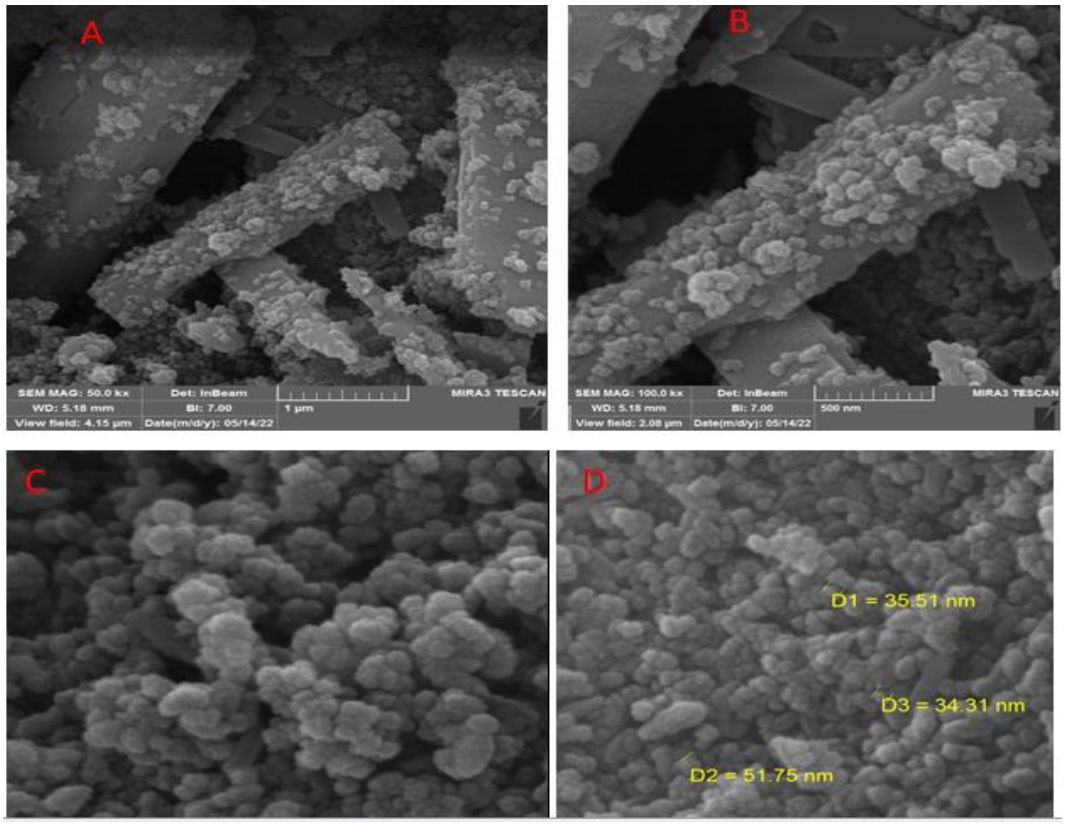

Figure 8: FE-SEM images of CuO/TiO_2 nanocomposite prepared by hydrothermal method at 400 C^o for 3h at PH=10.

3.3 TEM Analysis of CuO,TiO_2Nanopartecles and CuO /TiO_2 Nanocomposites

TEM images of copper oxide nanoparticles CuO NPs prepared using the hydrothermal method at 100 C^o for 2h at PH=10, as shown in Figure 9 (A-D), where the microscopic images confirm the formation of spherical nanoparticles, since the fission process took place in a free medium without any capping factor, some particles were overlapping among themselves, as it was noted that some spherical nanoparticles appear in a small size due to the phenomenon of agglomeration. The average size of copper oxide nanoparticles was 25 to 50 nm. [22]**.** TEM images of Titainum oxide nanoparticles (TiO_2) NPs prepared using the hydrothermal method at 400 ^oC for 2h at PH=8, as shown in Figure 10(A-D). The microscopic images confirm the formation of hexagonal nanoparticles, since the fission process took place in a free medium without any capping factor. Some particles were overlapped among themselves, as it was noted that some spherical nanoparticles appear in a large size due to the phenomenon of agglomeration. The average grain size of TiO_2 nanoparticles was 23 to 49 nm [23]. In addition, TEM was used to analyze the CuO/TiO_2 nanocomposite, providing insight into its internal shape and average grain sizes. Hydrothermal treatment was used to pre-crush the micron granules into finer particles. It is clear from Figure 11(A-D) that there were several gray particles present, along with a few darker patches. Microscopic evidence shows that the nanocomposite is spherical and that their average grain size is between 25 to 55 nm [24].

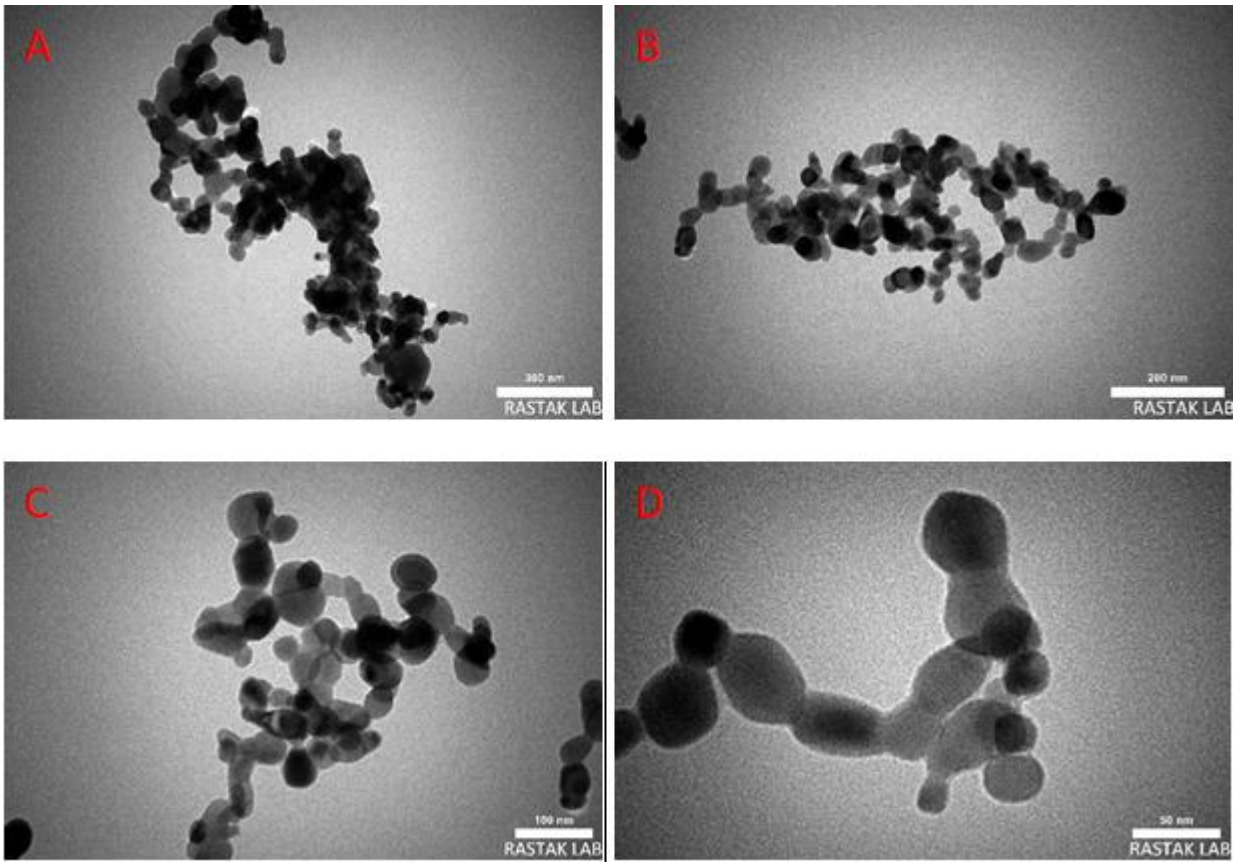

Figure 9: TEM images of CuO NPs prepared by hydrothermal method**.**

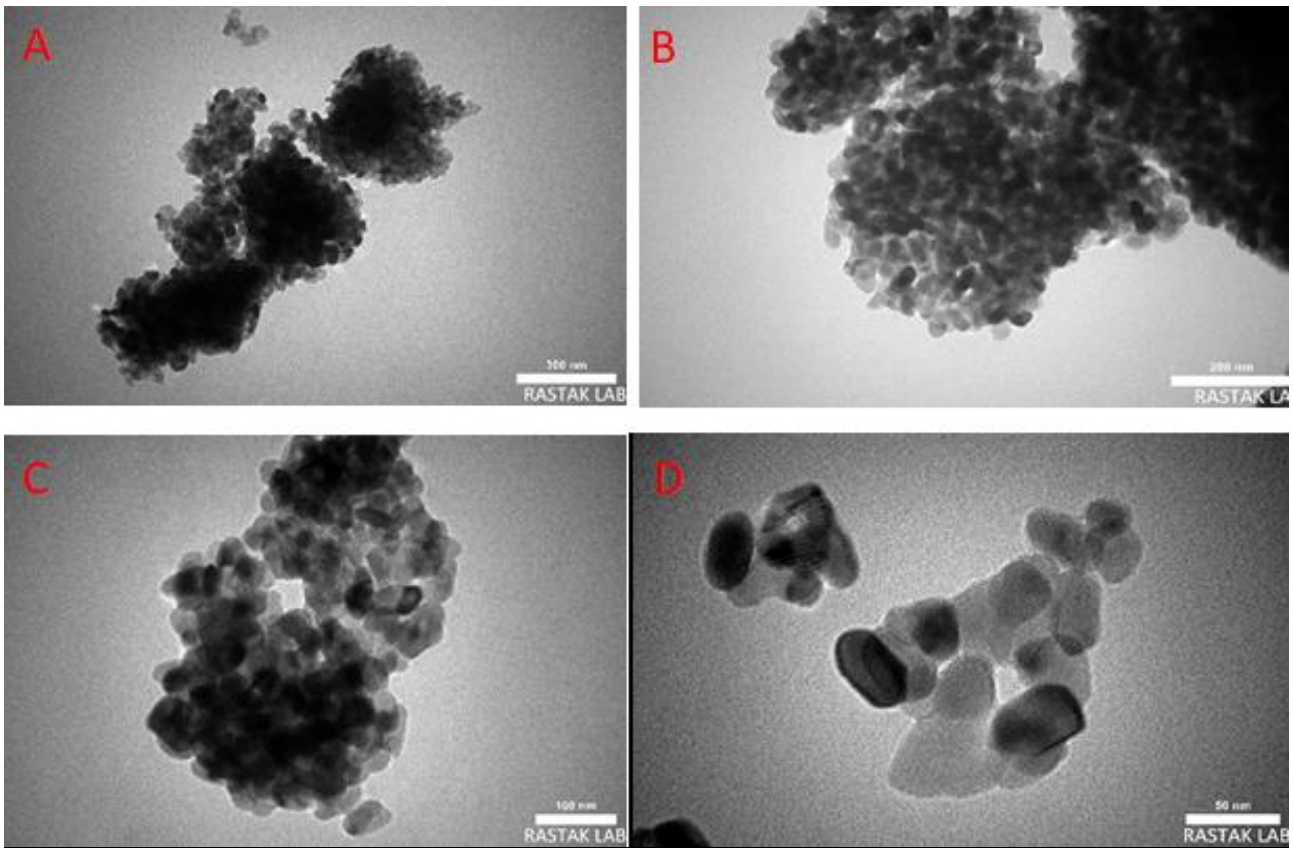

Figure10: TEM images of TiO_2 NPs prepared by hydrothermal method.

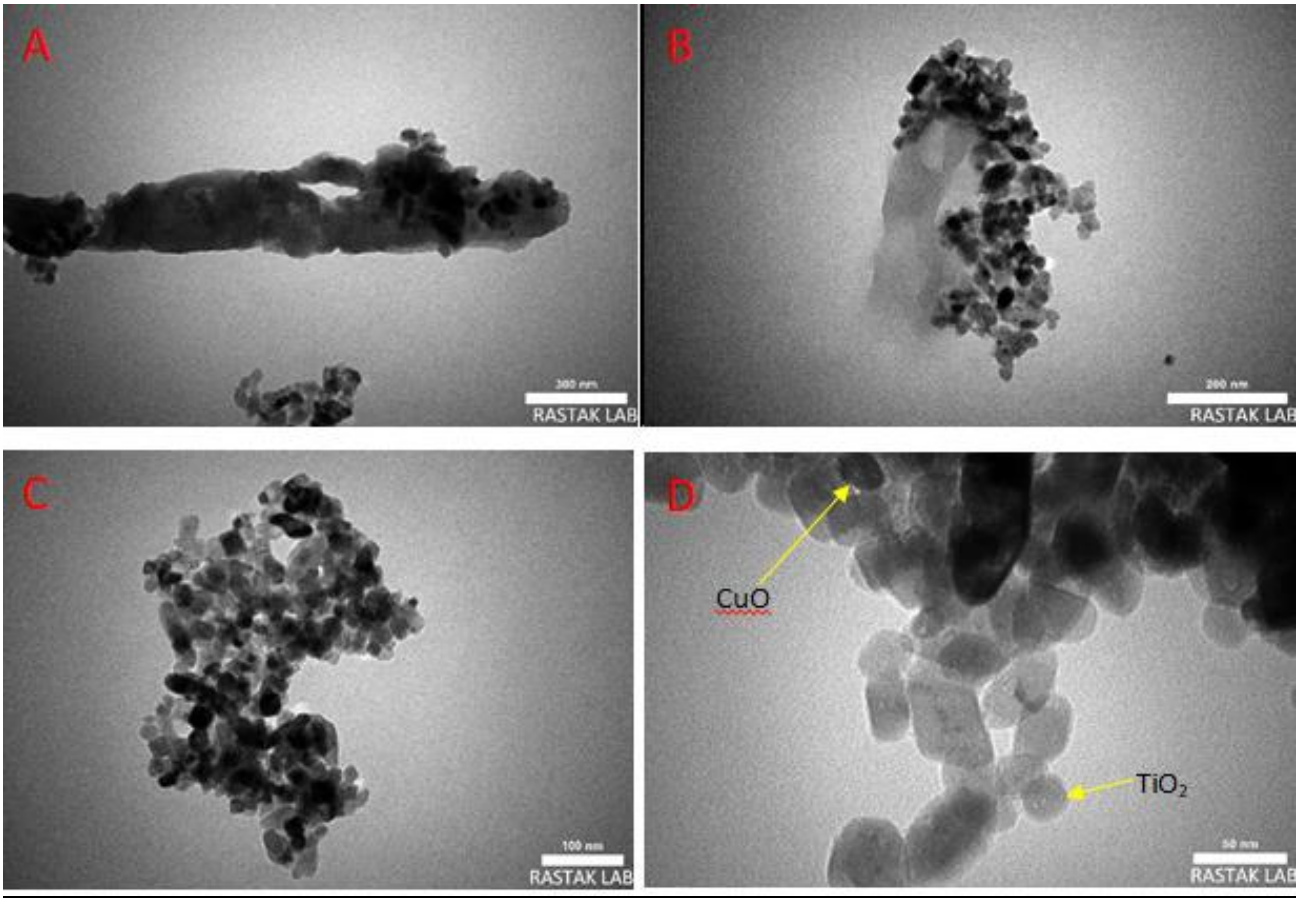

Figure 11: TEM images of CuO/TiO_2 nanocomposite prepared by hydrothermal method**.**

3.4 Optical Properties

The absorption spectra and energy band gab CuO, TiO_2 nanoparticles and CuO /TiO_2 nanocomposites are shown in Figures.(12-14) respectively and the Table 1.

Table 1: shows the energy band gap of CuO, ,TiO_2 and CuO/TiO_2.

CuO	2.1 eV
TiO_2	3.0 eV
CuO /TiO_2	2.8 eV

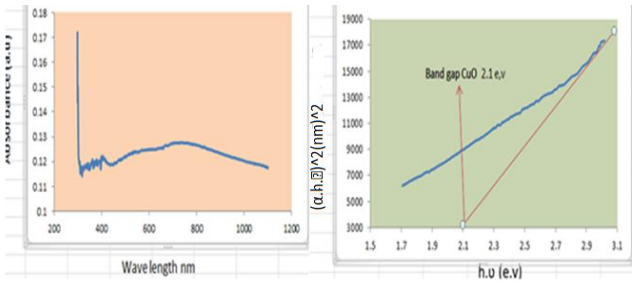

Figure12: The absorbance spectrum and optical band gap of CuO nanoparticles**.**

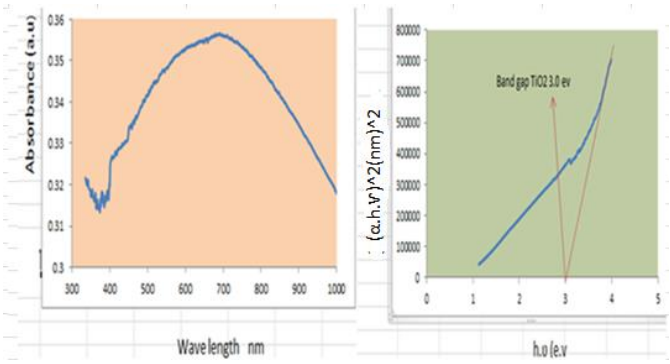

Figure 13: The absorbance spectrum and optical band gap of TiO_2 nanoparticles.

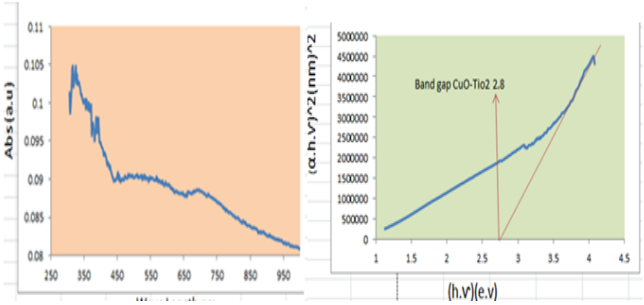

Figure 14: The absorbance spectrum and optical band gap of CuO/TiO_2 nanocomposite.

Fabricated dye-sensitized solar cells results

DSSCs are fabricated using TiO_2, CuO nanoparticles and CuO /TiO_2 nanocomposites as photoelectrode and two natural dyes, red pomegranate dye and green leek dye were used as an absorbent medium. Figures15(A,B,C) show the I-V characteristics of DSSCs prepared based on TiO2, CuO nanoparticles and CuO/TiO_2 nanocomposites / green leek dye has given V_{OC}, I_{SC} and efficiency (η%) are shown in a Table (2).

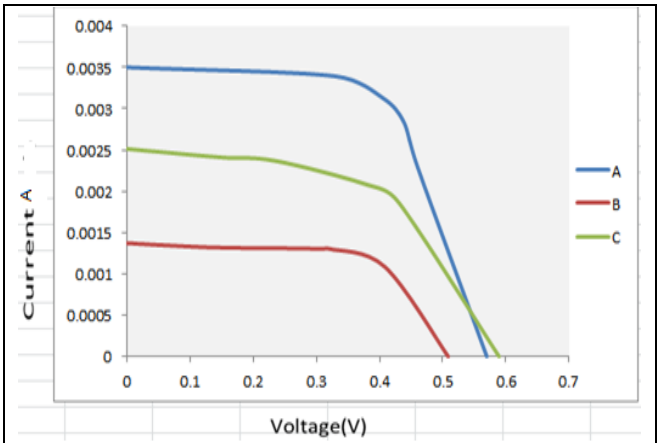

Figure15: I-V characteristics of prepared DSSCs, (A)CuO, (B) TiO_2 and(C) CuO/ TiO_2/ green leek dye.

Table2.Photo electrochemical parameters of the DSSCs, A=0.25cm^2 under intensity light28.2 Mw/cm ^{2} using/ green leek dye.

Catalyst/ gree n .leek dye	I_{SC} mA	V_{OC} (V)	I_{max} Ma	V_{max} (V)	P_{max}	FF%	%η
TiO_2	1.31	0.507	1.08	0.45	0.621	73	0.74
CuO	4.10	0.498	3.08	0.314	0.961	47	1.51
CuO/ TiO_2	2.5	0.599	1.8	0.431	0.743	40	0.94

Figures16 (A,B,C) show the I-V characteristics of DSSCs prepared based TiO_2,CuO nanoparticles, and CuO/TiO_2 nanocomposites/red pomegranate dye has given V_{OC} , ISC and efficiency (η%) are shown in a table(3).

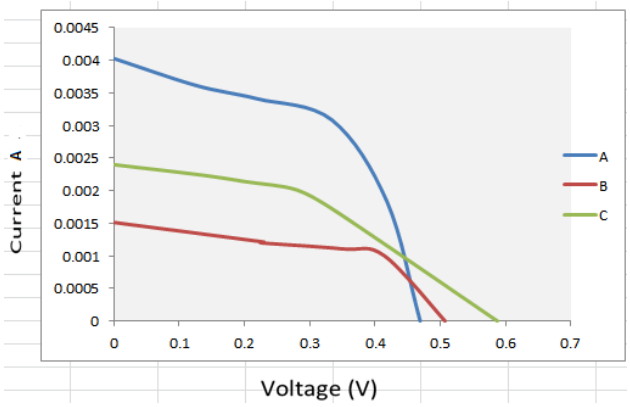

Figure16: I-V characteristics of prepared DSSCs, (A)CuO, (B) TiO_2 and(C) CuO/ TiO_2/ red pomegranate dye

Table.3: Photo electrochemical parameters of the DSSCs, A=0.25cm^2 under intensity light28.2 M w/cm^2 using red pomegranate dye.

Catalyst// red pomegranate .dye	I_{SC} mA	V_{OC} (V)	I_{max} mA	V_{max} (V)	P_{max}	FF%	**η%**
TiO_2	1.32	0.408	1.00	0.354	0.354	66	0.558
CuO	4.03	0.488	3.08	0.334	1.02	54	1.20
CuO/ TiO_2	2.4	0.587	1.69	0.338	0.193	40	0.88

The results showed that the efficiency of DSSC made on the basis of Cuo with green leek dye and red pomegranate dye is higher than that of TiO_2 NPs and CuO/TiO_2 nanocomposites. For many reasons. First, it has a low energy gap 2.1 ev in CuO. As the energy gaps decrease the efficiency increases. This is because lower energy gaps enable electrons with lower excitation energy to become free electrons in a conduction band and thus increase solar energy efficiency [25],[26]. Second, the surface area of CuO is 38.70 m^2/g and is higher than that of TiO_2 NPs and CuO/TiO_2 nanocomposites, which indicates an increase in dye adsorption on the surface of CuO this may lead to an increase in the efficiency of the fabricated DSSC[27]. In addition, the current yield of DSSCs with natural dye pomegranate red dye was lower than that of DSSCs made using leek green dye due to the dye in leek is a chlorophyll dye, which has an excess of electrons and can supply these electrons to the cell more effectively than the anthocyanin dye found in red pomegranate [28]. Moreover, the lower value achieved from the manufactured DSSCs is also a result of the light source's low density 28.2 mW/cm^2.

4. CONCLUSIONS

CuO, TiO_2 NPs and CuO/TiO_2 nanocomposite are prepared by hydrothermal method, it is very simple, fast, cost-effective, and environmentally. Semiconductor deposition on FTO glass by doctor blade gives a better homogeneous surface than dropping and evaporation of semiconductor solution suspended on FTO Similarly, deposited graphite gave a homogeneous and more stable surface than using candle flame which is quickly removed from a glass surface. Several techniques have been used to describe the products equipped with field emission scanning electron microscopy FE-SEM, transmission electron microscopy TEM and X-ray diffraction. It is noted from the previous data that the dye has a very important role in improving the efficiency of the solar cell, as the results showed that the cells made of the green leek chlorophyll dye produce a much higher efficiency than the cells prepared from the anthocyanin dye. The results also showed that the cells prepared from CuO NPs had better efficiency than TiO_2 NPs and CuO/TiO_2 Nanocomposite. As-prepared CuO,TiO_2 NPsand CuO/TiO_2 nanocomposite shows the fast electron transfer between n- and p-type semiconductors, which can be used for future applications such as sensor, biosensor, photocatalysis and solar cell.

5. REFERENCES

[1] Wiechec-Cudak, O., et al., Interactions of a Water-Soluble Glycofullerene with Glucose Transporter 1. Analysis of the Cellular Effects on a Pancreatic Tumor Model. Nanomaterials 2021, 11, 513. 2021, s Note: MDPI stays neutral with regard to jurisdictional claims in published ….

[2] Baig, N., I. Kammakakam, and W. Falath, Nanomaterials: A review of synthesis methods, properties, recent progress, and challenges. Materials Advances, 2021. 2(6): p. 1821-1871.

[3] Grätzel, M., Conversion of sunlight to electric power by nanocrystalline dye-sensitized solar cells. Journal of Photochemistry and Photobiology A: Chemistry, 2004. 164(1-3): p. 3-14.

[4] Cavallo, C., et al., Nanostructured semiconductor materials for dye-sensitized solar cells. Journal of Nanomaterials, 2017. 2017.

[5] Satari, C., et al., Literature review: synthesis of CuO (Copper Oxide) nanoparticles for thermal energy storage.

[6] Humayun, M., et al., Au surface plasmon resonance promoted charge transfer in Z-scheme system enables exceptional photocatalytic hydrogen evolution. Applied Catalysis B: Environmental, 2022. 310: p. 121322.

[7] Nasir, A., et al., A Review on the Progress and Future of TiO2/Graphene Photocatalysts. Energies, 2022. 15(17): p. 6248.

[8] Francis, O.I. and A. Ikenna, Review of dye-sensitized solar cell (DSSCs) development. Natural Science, 2021. 13(12): p. 496-509.

[9] Bera, S., et al., Research into dye-sensitized solar cells: a review highlighting progress in India. Journal of Physics: Energy, 2021. 3(3): p. 032013.

[10] Abd, M.A., R.M. Al-haddad, and K.H. Razeg, Synthesis and Characterization of copper oxide (II) nanoparticles prepared by hydrothermal process. Journal of University of Babylon for Pure and Applied Sciences, 2019. 27(4): p. 266-273.

[11] Yazid, S.A., Z.M. Rosli, and J.M. Juoi, Effect of titanium (IV) isopropoxide molarity on the crystallinity and photocatalytic activity of titanium dioxide thin film deposited via green sol–gel route. Journal of Materials Research and Technology, 2019. 8(1): p. 1434-1439.

[12] Santhi, K., et al., Synthesis and characterization of TiO2 nanorods by hydrothermal method with different pH conditions and their photocatalytic activity. Applied Surface Science, 2020. 500: p. 144058.

[13] Aljumaili, M., A. Abdalkafor, and M. Taha, Analysis of the Hard and Soft Shading Impact on Photovoltaic Module Performance Using Solar Module Tester. International Journal of Power Electronics and Drive Systems, 2019. 10.

[14] Padil, V.V.T. and M. Černík, Green synthesis of copper oxide nanoparticles using gum karaya as a biotemplate and their antibacterial application. International journal of nanomedicine, 2013. 8: p. 889.

[15] Wang, Y., et al., New insights into fluorinated TiO 2 (brookite, anatase and rutile) nanoparticles as efficient photocatalytic redox catalysts. RSC advances, 2015. 5(43): p. 34302-34313.

[16] Singh, A., et al., Structural, morphological, optical and photocatalytic properties of green synthesized TiO2 NPs. Current Research in Green and Sustainable Chemistry, 2020. 3: p. 100033.

[17] Reveendran, R. and M.A. Khadar. Synthesis, characterization and electrical properties of α-Fe2O3/CuO

nanocomposites. in AIP Conference Proceedings. 2019. AIP Publishing LLC.

[18] Van Tran, C., et al., Facile fabrication and characterizations of nanostructured Fe2O3-TiO2 composite from Ilmenite ore. International Journal of Advanced Engineering, Management and Science. 4(7): p. 264310.

[19] Abid, M.A., et al., Iron oxide nanoparticles synthesized using garlic and onion peel extracts rapidly degrade methylene blue dye. Physica B: Condensed Matter, 2021. 622: p. 413277.

[20] Gao, Y., et al., Construction of Fe2O3@ CuO heterojunction nanotubes for enhanced oxygen evolution reaction. ACS Applied Energy Materials, 2019. 3(1): p. 666-674.

[21] Danish, E.Y., et al., Adsorptive removal of lanthanum based on hydrothermally synthesized iron oxide-titanium oxide nanoparticles. Environmental Science and Pollution Research, 2020. 27(5): p. 5408-5417.

[22] Bhosale, M.A., et al., Magnetically separable γ-Fe2O3 nanoparticles: An efficient catalyst for acylation of alcohols, phenols, and amines using sonication energy under solvent free condition. Journal of Molecular Catalysis A: Chemical, 2015. 404: p. 8-17.

[23] Liu, Z. and C. Zhou, Improved photocatalytic activity of nano CuO-incorporated TiO2 granules prepared by spray drying. Progress in Natural Science: Materials International, 2015. 25(4): p. 334-341.

[24] Aleksić, O.S., et al., Structural and electronic properties of screen-printed Fe2O3/TiO2 thick films and their photoelectrochemical behavior. Journal of Materials Science, 2017. 52(10): p. 5938-5953.

[25] Elhouri, S.A., The Value of Efficiency and Energy Gap for Different Dye Solar Cells. Global Journal of Engineering Science and Researches, 2018. 5(8): p. 115-121.

[26] Contreras, M.A., et al. Improved energy conversion efficiency in wide bandgap Cu (In, Ga) Se 2 solar cells. in 2011 37th IEEE Photovoltaic Specialists Conference. 2011. IEEE.

[27] Son, Y.J., et al., Influence of TiO2 particle size on dye-sensitized solar cells employing an organic sensitizer and a cobalt (III/II) redox electrolyte. The Journal of Physical Chemistry C, 2018. 122(13): p. 7051-7060.

[28] Elsay, E.I.I., et al., Determination of Energy Gap & Efficiency in Dye Polymer Solar Cells. International Journal of Current Engineering and Technology, 2015. 5(4): p. 2713-2715.